Metallophysics and Advanced Technologies
Металофіз. новітні технол.
Metallofiz. Noveishie Tekhnol.
2023, vol. 45, No. 4, pp. 523–535
https://doi.org/10.15407/mfint.45.04.0523
Reprints available directly from the publisher

PACS numbers: 43.20.Hq, 43.35.Cg, 61.72.Ff, 62.20.de, 62.20.dj, 62.65.+k, 62.80.+f

Ultrasonic Investigation of High-Entropy $Al_{0.5}CoCrCuFeNi$ Alloy at Low Temperature

V. S. Klochko, A. V. Korniyets, I. V. Kolodiy, O. O. Kondratov,
V. I. Sokolenko, V. I. Spitsyna, T. M. Tykhonovska, and N. A. Yayes

National Scientific Centre 'Kharkiv Institute of Physics and Technology'
of the National Academy of Sciences of Ukraine,
Akademichna Str., 1,
UA-61108 Kharkiv, Ukraine

The temperature dependence of the velocity propagation and the change in the attenuation of plane-polarized ultrasonic waves at a frequency of 50 MHz in the high-entropy $Al_{0.5}CoCrCuFeNi$ alloy is investigated, using the ultrasonic spectroscopy in the temperature range 77–300 K. As found, the acoustic-characteristics' anisotropy of the alloy is due to the growth texture. Significant attenuation of ultrasonic waves is revealed. Its temperature dependence is analysed. The effect of annealing on the studied acoustic characteristics is investigated. The estimate of values of the dynamic Young's modulus, shear modulus, bulk modulus, and Poisson's ratio is made.

Key words: high-entropy alloy, ultrasonic studies, anisotropy, elastic modulus.

В інтервалі температур 78–300 K методом ультразвукової спектроскопії проведено дослідження температурної залежности швидкости поширення та зміни затухання пласкополяризованих ультразвукових хвиль частотою у 50 МГц у високоентропійному стопі $Al_{0.5}CoCrCuFeNi$. Виявлено анізотропію акустичних характеристик стопу, зумовлену текстурою росту. Виявлено значне згасання ультразвукових хвиль, проаналізовано вплив температури на його зміну. Вивчено вплив відпалу на досліджувані акустичні характеристики. Виконано оцінку динамічних модулів Юнґа, зсуву, об'ємного модуля всебічного стиску та Пуассонового коефіцієнта.

Ключові слова: високоентропійний стоп, ультразвукові дослідження,

Corresponding author: Korniyets Anatolii Vasylyovych
E-mail: korniets@kipt.kharkov.ua

Citation: V. S. Klochko, A. V. Korniyets, I. V. Kolodiy, O. O. Kondratov,
V. I. Sokolenko, V. I. Spitsyna, T. M. Tykhonovska, and N. A. Yayes, Ultrasonic Investigation of High-Entropy $Al_{0.5}CoCrCuFeNi$ Alloy at Low Temperature, *Metallofiz. Noveishie Tekhnol.*, **45**, No. 4:523–535 (2023). DOI: 10.15407/mfint.45.04.0523

анізотропія, модулі пружности.

(Received 9 February, 2023; in final version, 28 February, 2023)

1. INTRODUCTION

Multicomponent high-entropy alloys (HEAs) attract special attention, since the concept of high mixing entropy opens new doors to the development of modern materials with unusual combinations of mechanical and functional characteristics that cannot be achieved by traditional microalloying based on one dominant element. The decrease in free energy contributes to the stabilization of solid solution, dispersion-strengthened structural states. Lattice distortion, due to the difference in the atomic radii of the substitution elements, leads to the emergence of a favourable set of properties, which include hardness, strength, heat resistance, corrosion resistance, wear resistance. This allows not only create unique structural materials, but also does not exclude the possibility to discover new phenomena in their properties that makes their further research topical.

As cast alloys of the Al_xCoCrCuFeNi system (x = 0.25–6 mole) with a phase composition based on simple f.c.c. and b.c.c. structures are the most studied among the high-entropy materials [1–13], they demonstrated unique properties of HEAs. However, at cryogenic temperatures data are insufficient. At the same time, information about the acoustic and elastic properties, which reflect the nature of the internal bonding forces in a crystal, is any single. Previously [9–11], low-temperature (4.2–320 K) studies of this alloy at a bending vibration frequency of 513 Hz revealed thermally activated relaxation processes caused by dislocations. The obtained values of the Young's modulus (194–182 GPa) agreed with the literature data for similar type alloys [2]. At the same time, the authors did not take into account the crystallographic texture, which is inevitably formed at creating alloy blanks using the argon-arc method with directed heat removal. Texture leads to property anisotropy. In this regard, it became necessary to develop studies of the low-temperature (77–300 K) properties of the $Al_{0.5}$CoCrCuFeNi alloy, using the resource of pulsed ultrasonic technology, which includes high frequencies (50 MHz), orientation and polarization of ultrasonic waves.

2. RESEARCH METHODS AND SAMPLES

Ultrasonic studies were carried out by the pulse bridge method,

which makes it possible to obtain the values of the propagation velocity ($V_{L,S}$) and the change in attenuation ($\Delta\beta_L$) of ultrasonic waves in a single experiment. The excitation of longitudinal (L) and shear (S) plane-polarized waves was created by broadband resonant lithium niobate piezoelectric transducers with 50±2 MHz an intrinsic resonant frequency. The acoustic contact 'piezoelectric transducer–sample' was achieved with silicone oil and honey. Excitation by a high-frequency pulse generator with constant amplitude (≅ 1.5 V) realized the mode of amplitude-independent ultrasonic attenuation. The measurements were carried out with ΔT = 1–2 K temperature interval in the samples warming up mode at a rate of 0.5 K/min. The temperature stabilization of the sample was kept at a level of ±0.05 K. The relative measurement error of V_L and β_L is of 10^{-6} and 10^{-3}, respectively. The measurement error caused by the binder liquids was of 0.5–1%. When $\Delta\beta_L$ was measuring, the insignificant contribution of the silicone binder softening to the change in the attenuation of longitudinal ultrasonic waves was not taken into account at $T > 120$ K.

Elastic characteristics were determined from experimental data of the velocity of longitudinal V_L and shear V_S ultrasonic waves propagation and density ρ according to the known relations:

$$E = \rho V_S^2 \frac{3V_L^2 - 4V_S^2}{V_L^2 - V_S^2}, \tag{1}$$

$$B = \rho(V_L^2 - \frac{4}{3}V_S^2), \tag{2}$$

$$G = \rho V_S^2, \tag{3}$$

$$\upsilon = \frac{V_L^2 - 2V_S^2}{2(V_L^2 - V_S^2)}, \tag{4}$$

where E is Young's modulus, B is the bulk modulus, G is the shear modulus, υ is the Poisson's ratio.

X-ray studies were carried out on a ДРОН-2 serial diffractometer in FeK_α radiation using a selectively absorbing manganese filter.

The original ingot of a multicomponent alloy, which consist of Al(4.46), C(19.48), Cu(21.01), C(17.18), Ni(19.4), Fe(18.46) wt.%, was obtained by remelting components (purity ≅ 99.9%) on a copper water-cooled hearth in an arc furnace using a non-consumable tungsten electrode. Remelting was carried out in the atmosphere of purified argon. To ensure uniform distribution of components, the alloy five times was remelted, with turnover on the hearth. The density of the alloy was of 7.979 g/cm^3.

Research samples (5.7×4×4 mm^3 (HEA1) and 5.5×4×4 mm^3

(HEA2) were cut from adjacent sections of the original billet ($7\times7\times30$ mm^3) using electric spark cutting. To obtain plane-parallel surfaces along (HEA2) and perpendicular (HEA1) to the heat removal direction, they were rubbed using abrasive materials.

The metallographic studies, which are shown in Fig. 1, indicate that the alloy microstructure has a typical dendritic character that consists of a body of dendrites (it is main part) and interdendritic spaces. It can be seen that, in the HEA1 sample (Fig. 1, *a*), the primary axis of the dendrites are oriented parallel to the heat removal direction, whereas, in HEA2 (Fig. 1, *b*), sections of the alloy surface are observed with the orientation of the dendrite axes both parallel and perpendicular to the direction of heat removal.

The alloy microhardness perpendicular to the dendrites primary axis was of 2500 MPa, in parallel, it is of 2300 MPa.

According to x-ray diffraction data, the branches of dendrites and interdendritic regions had f.c.c.$_1$ and f.c.c.$_2$ crystal structures with very close lattice parameters, while the ratio of the intensities of diffraction reflections indicates the presence of a predominant crystallite orientation in the samples. The results of x-ray studies are shown in Tables 1 and 2.

Previously obtained data of scanning electron microscopy using an x-ray microanalyser for the present alloy [9] show that the elemental composition of dendrites and interdendritic spaces is significantly different. According to the authors, the dendrites composition is enriched in iron, chromium, and cobalt by more than

TABLE 1. X-ray diffraction data of the HEA1 sample.

Phase	*hkl*	2θ angle, deg	Intensity, imp/sec	Lattice parameter *a*, Å
f.c.c.$_1$	111	55.46	391.7	3.599
	200	65.01	889.6	
	220	99.03	393.0	
	311	26.29	216.3	
f.c.c.$_2$	200	64.43	241.9	3.624
	220	97.88	63.3	
	311	124.76	72.9	

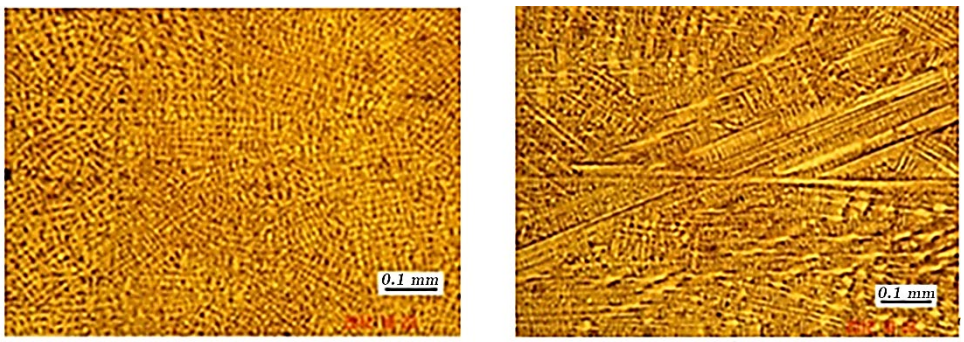

Fig. 1. Microstructure of high-entropy $Al_{0.5}CoCrCuFeNi$ alloy: (*a*) HEA1 sample, (*b*) HEA2 sample.

20 at.% of each element and depleted in copper and aluminium less than 10 at.%. The interdendritic spaces are enriched in copper up to ≅ 65 at.% and contain a small amount (less than 4 at.%) of iron, chromium, and cobalt. The aluminium content in the interdendritic spaces is greater (≅ 15 at.%), which, according to Ref. [1], leads to an increase in the f.c.c. lattice parameter. In addition, at the boundary between dendrites and interdendritic region, separate spaces are observed to be close in composition to the interdendritic region, but containing less copper and a higher amount of nickel, iron, chromium, and cobalt.

Thus, taking into account the ratio of the intensities of diffraction reflections in x-ray diffraction patterns and the estimation of the volume fraction of phases according to metallography data, dendrites correspond to a phase with a lower lattice parameter (f.c.c.$_1$) and interdendritic region corresponds to a phase, which has a larger lattice parameter (f.c.c.$_2$).

3. RESULTS AND DISCUSSION

Figure 2 presents data a longitudinal ultrasonic wave velocity $V_L(T)$ at 50 MHz frequency in the HEA1 sample (Fig. 2, *a*) and in the HEA2 sample (Fig. 2, *b*) in the temperature range from 78 to 300 K. In both cases, almost monotonically increasing dependence of $V_L(T)$ is observed with decreasing temperature. The difference in the absolute value of the ultrasound velocity is ≅ 4%, wherein, there is a slight difference in the slope of the $V_L(T)$ in the temperature range between 125 K and 300 K.

Cubic crystals are known [14] to constitute the $m3m$ elastic symmetry class; therefore, symmetry axes of $n > 2$ order are the

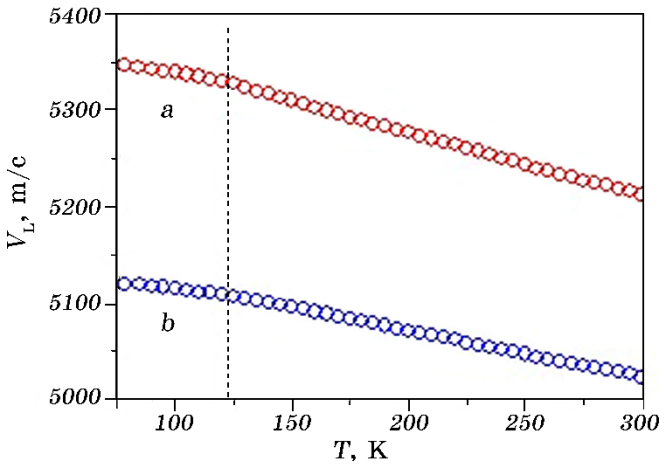

Fig. 2. Temperature dependences of the longitudinal ultrasonic wave velocity at 50 MHz frequency: (*a*) HEA1 sample, (*b*) HEA2 sample.

crystal acoustic axes. Since the HEA1 sample has a crystallites' predominant orientation in [100] direction (4-order symmetry axis), it is quite probably to assume that the temperature dependence of the longitudinal ultrasound velocity propagating in [100] direction is determined by dependence on temperature of the elasticity-tensor constant c_{11} of f.c.c. lattice as a result thermal expansion of the alloy.

Based on the ratios of the diffraction reflections intensities, the HEA2 sample for the f.c.c.$_1$ phase has an insignificant predominant

TABLE 2. Characteristics of used materials.

Phase	*hkl*	2θ angle, deg	Intensity, imp/sec	Lattice parameter *a*, Å
	111	55.593	624.7	
f.c.c.$_1$	200	65.110	164.5	3.594
	311	126.561	120.8	
	111	55.097	30.0	
f.c.c.$_2$	200	64.511	45.9	3.624
	311	124.757	38.4	

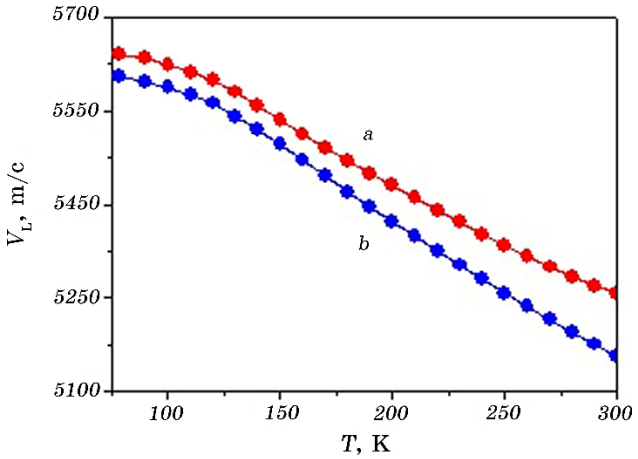

Fig. 3. Temperature dependences of the velocity of longitudinal ultrasonic wave at 50 MHz frequency in the samples of HEA1 (*a*) and HEA2 (*b*) after annealing at 1248 K for 12 h.

orientation of crystallites in [111] direction, while for the f.c.c.$_2$ phase, it is in [100] direction. Thus, Figure 2, *b* demonstrates the temperature dependence of the quasi-longitudinal ultrasonic wave velocity, which is determined by the contribution of all independent constants of the f.c.c. lattice elastic tensor during thermal expansion. In the vicinity of $\cong 120$ K, both $V_L(T)$ dependences exhibit a characteristic flexure due to the phonon spectrum softening, through developing relaxation processes of phonon scattering [15].

The elastic characteristics are known mainly to reflect the short-range order of interatomic interaction. Therefore, an important peculiarity affecting their magnitude and, hence, the magnitude of the ultrasound velocity is the atoms' compositional surrounding of the first co-ordination sphere. In this case, of course, one must also take into account the electronic structure of the alloy, namely, the presence of a covalent-like chemical bond arising in the alloy as a result of the electronic-orbitals' hybridization of the atoms of its components.

After annealing at 1248 K for 12 hours, followed by slow cooling, the dependences $V_L(T)$ (Fig. 3) undergo significant changes. First, for both samples, an increase in the velocity value is observed ($\cong 5\%$ at a temperature of 78 K and $\cong 1\%$ at $T = 300$ K), wherein the $V_L(T)$ for HEA1 (Fig. 3, *a*) demonstrates a characteristic flexure that suggests the development of thermally activated structural processes. Secondly, the anisotropy of this parameter is practically absent. In contrast to the $V_L(T)$ dependences for the original

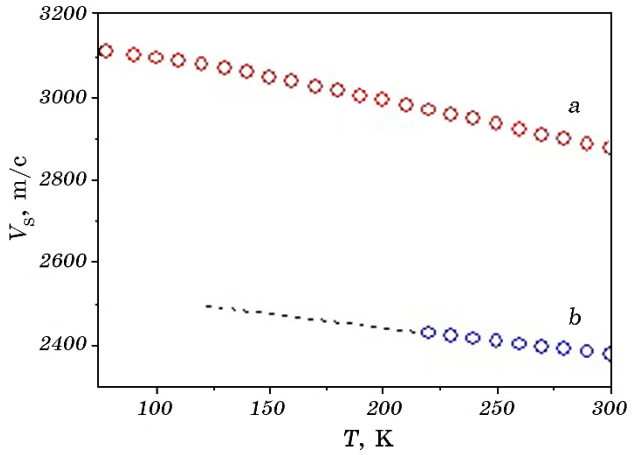

Fig. 4. Temperature dependences of the velocity of shear ultrasonic wave at 50 MHz frequency: (*a*) HEA1 sample, (*b*) HEA2 sample.

samples, where the anisotropy degree somewhat is increased as temperature is decreased, the alloy becomes practically isotropic with decreasing of temperature for annealed samples. It is obvious that this is caused by a change in the state of the alloy structural–phase composition.

Scanning electron microscopy data using an x-ray microanalyser [9] show that the dendritic-regions' composition remains practically unchanged, while, in the interdendritic regions, the copper and aluminium contents are decreased, and other elements' content is increased. Mostly at the boundaries between dendritic and interdendritic regions, the formation of sites enriched with nickel ($\cong$ 30%), aluminium (> 20%) and copper (> 20%) occurs. In addition, because of structural–phase transformations, the b.c.c. phase is also released in the f.c.c. matrix.

Figure 4 shows the temperature dependence of the velocity of shear ultrasonic waves $V_S(T)$ at 50 MHz frequency in a HEA1 sample (Fig. 4, *a*) and HEA2 (Fig. 4, *b*). Since in HEA1 sample (Fig. 4, *a*) the direction of sound propagation coincides (or is rather close) with the acoustic axis, the change in the sound velocity is determined by a temperature dependence of the elastic-tensor constant c_{44}. When the direction of the polarization vector of the shear ultrasonic wave was changed, the velocity value changed insignificantly ($\cong$ 1.5–2%), taking into account the error $\cong$ 1%, which was introduced by the acoustic contact (gluing). This fact indicates the presence of <100> axial texture in the HEA1 sample, which was formed in the alloy during crystallization. When the velocity of shear ultrasonic waves was measuring in HEA2 sample (Fig. 4, *b*), a critical decrease of the

TABLE 3. Elastic characteristics of high-entropy $Al_{0.5}CoCrCuFeNi$ alloy at 300 K. E is Young's modulus, G is shear modulus, B is bulk modulus, υ is Poisson's ratio.

Simple	Elastic characteristics			
	E, GPa	G, GPa	B, GPa	υ
HEA1	175.6	69.4	124.1	0.26
HEA2	122.3	45.1	141.2	0.36

ultrasonic wave amplitude was observed in the temperature range 78–215 K. Simultaneously, a noticeable difference in the magnitude of the ultrasound velocity was noted to be depending on the orientation of the polarization vector relative to the direction of the primary axes of the dendrites. In this case, the maximum difference in the V_S value at room temperature was ≅ 10%. The difference in the values of shear wave velocity for the samples is ≅ 20%.

When $V_S(T)$ of annealed samples was measuring, extremely low amplitude of the ultrasonic wave was noted due to the scattering of sound on structural inhomogeneities comparable with the wavelength, the density of which increased because of a change in the alloy morphology. This prevented further research.

Based on experimental data on the velocity of longitudinal and shear ultrasonic waves and the density of the origin samples, effective dynamic elastic moduli and Poisson's ratios were determined using Eqs. (1)–(4). The results obtained at 300 K are shown in Table 3. As can be seen, the values of the elastic characteristics for the HEA1 and HEA2 samples are noticeably differ due to the certain elastic anisotropy, which is also supplemented by the spatial heterogeneity of this material [12].

Since the alloy has a texture, it is useful to have information about its elastic characteristics parallel the texture axis.

Table 4 shows the HEA1 sample data (at 300 K) obtained using known relations for cubic crystals:

$$\rho V_{L[100]}^2 = c_{11},\ \rho V_{S[100]}^2 = c_{44},\ G_{[100]} = c_{44},$$
$$E_{[100]} = (c_{11} - c_{12})(c_{11} + 2c_{12})/(c_{11} + c_{12}).$$

The elasticity constant c_{12} is determined by the mixture rule [16]:

$$M = \frac{\sum c_i V_i M_i}{\sum c_i V_i}, \tag{5}$$

where c_i is the atomic part, V_i is molar volume, M_i is elasticity-tensor constant c_{12} of the alloy according to known data of alloy

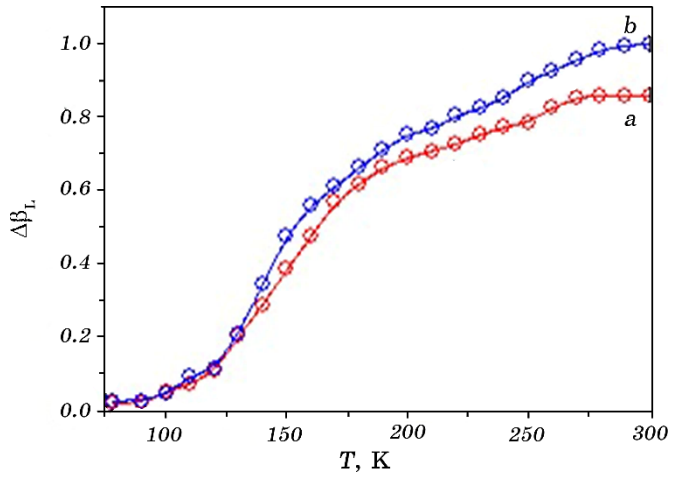

Fig. 5. Temperature dependence of the change in the attenuation of longitudinal ultrasonic waves at 50 MHz frequency normalized to $\Delta\beta_{max}$ of HEA1 (*a*) and HEA2 (*b*) samples.

components equal to 60.9(Al), 138.1(Fe), 165(Co), 160(Ni), 124(Cu), 59(Cr) GPa.

Figure 5 shows the temperature dependence of the change in the attenuation of longitudinal ultrasonic waves $\Delta\beta_L(T)$ in the HAE1 (Fig. 5, *a*) and HEA2 (Fig. 5, *b*) samples. As can be seen, both curves have a typical *S*-shape due to the intensification of the relaxation processes of phonon scattering known as Akhiezer's losses [15].

Noteworthily, it is the significant background attenuation of ultrasonic waves caused by both absorption (internal friction) and scattering of the ultrasonic wave on the inhomogeneities of the dendritic structure, which differ by compressibility, since the densities of the alloy components (the exception is Al) differ insignificantly remaining within 7.19(Cr)–7.87(Fe)–8.9(Co, Cu, Ni) g/cm^3. Consequently, when an ultrasonic wave propagates in an alloy, elastic pulsations are also possible.

After annealing at 1248 K for 12 hours, $\Delta\beta_L(T)$ for the HEA1 sample (Fig. 6, *a*) demonstrates an extreme dependence in the vicinity of a temperature of $\cong$ 170 K, while $\Delta\beta_L(T)$ for the HEA2 sample (Fig. 6, *b*) remains virtually unchanged except for a slight increase in the slope. The change in the dislocation structure of the alloy because of annealing caused the appearance of an acoustic attenuation peak in $\Delta\beta_L(T)$ in the vicinity of $T \cong 170$ K.

The estimation of the activation energy based on the width of the peak at half its height is determined according to the relationship

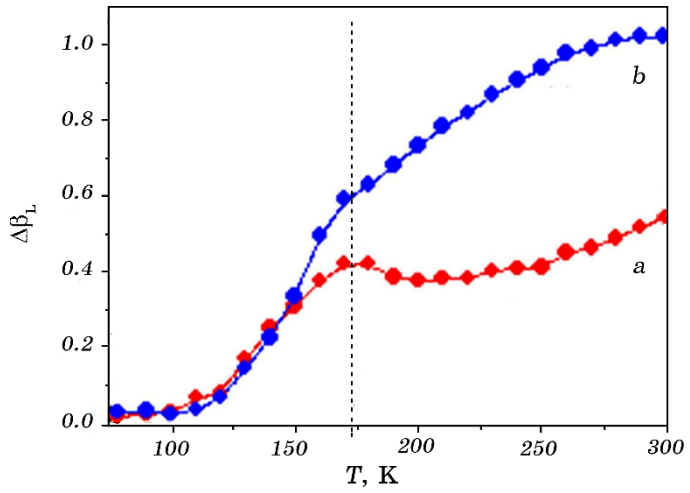

Fig. 6. Temperature dependence of the change in the attenuation of longitudinal ultrasonic waves at 50 MHz frequency normalized to $\Delta\beta_{max}$ of HEA1 (*a*) and HEA2 (*b*) samples after annealing at 1248 K for 12 h.

[17]:

$$E_a = 2.63R\frac{T_1T_2}{T_2 - T_1}, \tag{6}$$

where R is the molar gas constant, T_1 and T_2 are the temperatures of the peak at half height, and is $\cong 0.1$ eV, which is characteristic of a relaxation resonance of the Bordoni type observed in monoatomic materials.

Relaxation resonance due to the viscous motion of dislocations (of the Hasiguti type) was observed in an annealed alloy of a similar composition at a bending vibration frequency of 513 Hz [9]. Its detailed statistical and thermal activation analysis [10, 11] was considered based on the nonconservative viscous dislocation motion observed in f.c.c. metals.

The absence of relaxation resonance in the annealed HEA2 sample is apparently associated with the absence of certain (in magnitude and direction in the alloy) shear stresses in the easy-slip plane of dislocations due to the difference in the orientation of the ultrasound polarization vector relative to easy-slip directions in the samples.

However, another explanation for the extreme dependence $\Delta\beta_L(T)$ is also possible due to martensitic transformation, the temperature of which is sensitive to the elemental composition of the alloy [18]. Confirmation or refutation of this requires further precision

studies.

4. CONCLUSIONS

As a result of studies at low and moderately low temperatures (77–300 K) of the propagation velocity and changes in the attenuation of ultrasonic waves at 50 MHz in high-entropy $Al_{0.5}CoCrCuFeNi$ alloy, the following was established.

1. Anisotropy of the propagation velocity of longitudinal (4%) and shear (20%) ultrasonic (50 MHz) waves and the corresponding elastic characteristics is observed, which is due to the growth texture. Its decrease (up to $\cong 1.5\%$ for V_L) is associated with a change in the state of the alloy structural–phase composition because of annealing at $T = 1248$ K.

2. Significant attenuation of ultrasonic waves is due to both internal friction and scattering on structural inhomogeneities comparable with the ultrasonic wavelength.

The peak of acoustic attenuation at $\cong 170$ K in the alloy annealed at $T = 1248$ K is caused by the development of relaxation processes of the Bodoni type ($E_a \cong 0.1$ eV).

REFERENCES

1. C. J. Tong, Y. L. Chen, J. W. Yeh, S. J. Lin, and S. K. Chen, *Metall. Mater. Trans. A*, **36**: 881 (2005).
2. L. H. Wen, H. C. Kou, J. S. Li, H. Chang, X. Y. Xue, and L. Zhou, *Intermetallics*, **17**, Iss. 4: 266 (2009).
3. Che-Wei Tsai, Ming-Hung Tsai, Jien-Wei Yeh, and Chih-Chao Yang, *J. Alloys Compd.*, **490**, Iss. 1–4: 160 (2010).
4. S. Sing, N. Wanderka, B. S. Murty, U. Glatzel, and J. Banhart, *Acta Mater.*, **59**, Iss. 1: 182 (2011).
5. Chun Ng, Sheng Guo, Junhua Luan, Sanqiang Shi, and C. T. Liu, *Intermetallics*, **31**: 165 (2012).
6. X.-W. Qiu, *J. Alloys Compd.*, **555**: 246 (2013).
7. M. Tsai and J. Yeh, *Mater. Res. Lett.*, **2**, No 3: 107 (2014).
8. M. V. Ivchenko, V. G. Pushin, and N. Wanderka, *Zhurnal Tekhnicheskoi Fiziki*, **84**, No. 2: 57 (2014) (in Russian).
9. Yu. A. Semerenko, E. D. Tabachnikova, T. M. Tikhonovskaya, I. V. Kolodiy, A. S. Tortika, S. G. Shumilin, and M. A. Laktionova, *Metallofiz. Noveishie Tekhnol.*, **37**, No. 11: 1527 (2015) (in Ukrainian).
10. E. D. Tabachnikova, M. A. Laktionova, Yu. A. Semerenko, S. G. Shumilin, and A. V. Podolsky, M. A. Tikhonovsky, J. Miskuf, and K. Csach, *Low Temp. Phys.*, **43**, No. 9: 1108 (2017).
11. Yu. A. Semerenko and V. D. Natsik, *Low Temp. Phys.*, **46**, No. 1: 92 (2020).
12. V. M. Nadutov, O. I. Zaporozhets, N. A. Dordienko, V. A. Mikhaylovsky, S. Yu. Makarenko, and A. V. Proshak, *Fizika i Tekhnika Vysokikh Davleniy*,

26, Nos. 3–4: 31 (2016) (in Ukrainian).
13. V. N. Voyevodin, V. A. Frolov, E. V. Karaseva, A. V. Mats, V. I. Sokolenko, T. M. Tikhonovskaya, and A. S. Tortika, *Functional Materials*, **46**, No. 4: 683 (2021) (in Ukrainian).
14. Yu. I. Sirotin and M. P. Shaskolskaya, *Osnovy Kristallografii* [Fundamentals of Crystallography] (Moskva: Nauka: 1975) (in Russian).
15. *Ultrazvukovyye Metody Issledovaniya Dislokatsiy: Sb. Statei* [Ultrasonic Methods for Studying Dislocations] (Ed. L. G. Merkulov) (Moskva: Izd. Inostr. Lit.: 1963), p. 321 (Russian translation).
16. W. J. Wang, *Progress in Materials Science*, **57**, No. 3: 487 (2012).
17. V. S. Postnikov, *Vnutrenneye Trenie v Metallakh* [Internal Friction in Metals] (Moskva: Metallurgiya: 1974), p. 301 (Russian).
18. H. Y. Kim, I. Ikehara, L. I. Kim, H. Hosoda, and S. Miyazaki, *Acta Matter.*, **54**, No. 9: 2419 (2006).